Validation of a Power Transformer Model for Ferroresonance with System Tests on a 400 kV Circuit

Charalambos Charalambous[1], Z.D. Wang[1], Jie Li[1], Mark Osborne[2] and Paul Jarman[2]

Abstract-- National Grid has performed in the past a number of switching tests on a circuit configuration which was known to exhibit ferroresonance. The aim of the tests was to establish the likelihood of ferroresonance and quantify the effect on switchgear due to the de-energisation of a power transformer attached to a long over head line circuit. This paper, describes and compares the modeling work carried out in ATP (commercially available software) with the field ferroresonance test recordings. The accomplishment of a suitable simulation model will allow sensitivity studies to be carried out to determine the degree of influence of different components and parameters on the ferroresonance phenomenon.

Keywords: ATP, Ferroresonance, Power Transformer, Simulation Model, Field Tests.

I. Introduction

Certain circuit configuration of the UK transmission network provides an ideal environment for ferroresonance to occur. The possibility of Ferroresonance can be eliminated by the use of additional circuit brakers; however the economic justification needs to be carefully considered. Ferroresonance can be established when a transformer feeder circuit has been isolated, but continues to be energized through capacitive coupling to the energized parallel circuit [1].

A particular example is when one side of a double circuit transmission line connected to a transformer is switched out but remains capacitively energized, normally at a sub-harmonic frequency, because of coupling from the parallel circuit. Recovering from this condition requires the operation of a disconnector or earth switch on the resonating circuit, potentially resulting in arcing and damage, or switching off the parallel circuit resulting in an unplanned double circuit outage.

1. Charalambos Charalambous Zhongdong Wang and Jie Li are with the School of Electrical and Electronic Engineering, The University of Manchester, Manchester, M60 1QD, U.K (charalambos.charalambous@manchester.ac.uk, zhongdong.wang@manchester.ac.uk).

2. Mark Osborne and Paul Jarman are with National Grid, UK (mark.osborne@uk.ngrid.com, paul.jarman@uk.ngrid.com).

Presented at the International Conference on Power Systems Transients (IPST'07) in Lyon, France on June 4-7, 2007

Failing to detect or remove a ferroresonant condition can result in overheating of parts of the transformer as it is being repeatedly driven into magnetic saturation by the ferroresonance. Both instrument transformers and power transformers can be subject to ferroresonance.

In 1998 National Grid performed a number of switching tests on a circuit configuration which was known to exhibit ferroresonance.

This paper describes the modeling work carried out in ATP [2] (commercially available software) to reproduce the field ferroresonance tests performed. Furthermore, the accomplishment of a suitable simulation model will allow the authors to perform sensitivity studies to determine the degree of influence of different components and parameters on the ferroresonance phenomenon [3].

II. The 400kV double Circuit configuration

A. Physical Circuit Description and Testing

The Brinsworth/ Thorpe Marsh circuit was identified as a suitable circuit that could be induced to resonate, and that could be reasonably accessed. The purpose of the tests was to establish the likelihood of ferroresonance to occurring and the impact on the switchgear during quenching of the condition. [4].

Figure 1 illustrates a single line diagram of the Brinsworth/ Thorpe Marsh circuit arrangement. The length of the parallel overhead line circuit is approximately 37km and the feeder has a 1000 MVA 400/275/13 kV power transformer.

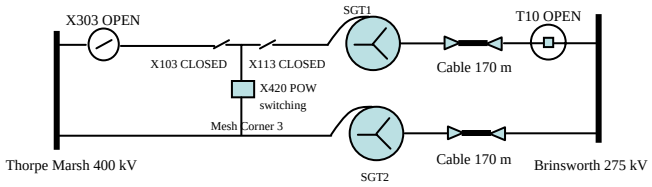

Fig. 1. Single line diagram of the Brinsworth / Thorpe Marsh circuit arrangement

It should be noted this is not a normal running arrangement, however to facilitate the testing this configuration was used on the day. The circuit equipment conditions prior to Ferroresonance testing are as follows: At Thorpe Marsh 400 kV substation side the disconnector X_{303} was locked open and mesh corner 3 restored to service. At

Brinsworth 275kV substation the circuit breaker T_{10} is open. At Brinsworth 400kV substation all disconnectors and circuit breaker X_{420} are in service. Point-on-wave (POW) switching was carried out on the Brinsworth/ Thorpe Marsh circuit using circuit breaker X_{420} to induce Ferroresonance. This type of switching prevents switching overvoltage conditions and provides a degree of controllability to the tests. The circuit breaker was tripped via an external POW control device.

After each switching operation the POW switching control was advanced by 1ms. At +3ms POW switching, a sub-harmonic mode ferroresonance was established, while at +11ms POW a fundamental mode ferroresonance was induced. The ferroresonance voltage and current waveforms available from field tests are illustrated in Appendix I .The waveforms presented correspond to the fundamental and subharmonic case.

B. Simulation Model Description

An ATP model has been developed to simulate the testing carried out on the circuit with the ultimate purpose to match field recordings that were available. Figure 2 illustrates a layout of the simulation model, which includes a description of the components of the model.

The main components of the network are: a parallel overhead line circuit (37 km) modeled considering the transmission line characteristics (typical overhead line spacings for a 400kV double circuit) [7], a transformer model utilizing the BCTRAN transformer matrix mode. Saturation effects have been considered by attaching the non- linear characteristics externally in the form of a non-linear inductive element branch.

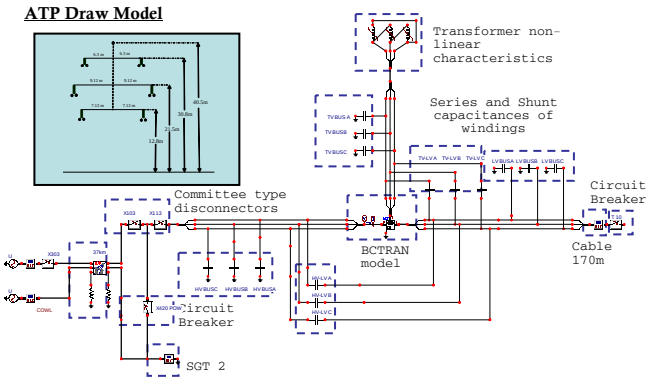

Fig. 2. Layout of ATPDraw simulation Model, including a description of the components characteristics utilized

Non-linear inductances can be modeled as a two slope piecewise linear inductances, with sufficient accuracy [2]. The slope in the saturated region above the knee reflects the air core inductance which is almost linear and low compared with the slope in the unsaturated region. The transformer magnetisation curve has been derived from manufacturer's data available and is illustrated by Table I.

For cylindrical coil construction, it is assumed that the flux in the winding closest to the core will mostly go through the core, since there should be very little leakage. This winding is usually the tertiary winding, and is therefore best to connect the nonlinear inductance across the tertiary terminals. Although attaching the non-linear effect externally is an approximation, it is reasonably accurate for frequencies below 1 kHz [5].

TABLE I
TRANSFORMER MAGNETIZING CHARACTERISTICS

Current (A)	Flux Linkage (Wb-turn)
7.18	48.77
7.85	52.02
8.35	55.27
19.37	58.52
35.40	61.77
78.48	65.02
222.09	65.92
5531.04	66.72

In low frequency transformer models is possible to represent each winding as one element. This does not come at the expense of accuracy. The model also comprises the interwinding and shunt capacitance elements, which have been calculated by employing mathematical methods taking into consideration the transformer equivalent circuit and the winding disc configurations types.

C. Transformer Characteristics and Data

The transformer characteristics available are tabulated in Table II.

TABLE II
TRANSFORMER CHARACTERISTICS

Rating	1000 MVA
Type	400/275/13 kV (auto)
Core Construction	Five Limb Core
Vector	Yy0
Bolt main:	No
Bolt Yoke:	No
% Ratio 4&5 \ Y \ M	60\60\100

The transformer has been modeled in the BCTRAN module of ATP draw which utilizes an admittance matrix representation of the form

$$[I] = [Y].[V] \qquad (1)$$

and in transient calculations can be represented as

$$[\frac{di}{dt}] = [L]^{-1}[v] - [L]^{-1} \cdot [R][i] \qquad (2)$$

The elements of the matrices are derived from open circuit and short circuit tests that are made in the factory. The data used in this simulation model include impedances and losses averaged for the test results of 8 transformers rated at1000 MVA (400/275/13 kV). Saturation effects have been modeled externally as previously described.

The impedances and load losses can only be measured for

winding pairs, but the designed load capability for the tertiary winding of this 1000 MVA design is only 60 MVA compared with the 1000 MVA throughput for the HV and LV terminals. Thus the H-T and L-T losses and impedances would be measured at 60 MVA. For this simulation model data a common base load is chosen to be 1000 MVA.

In service, the tertiary load would never be above 60 MVA if it was loaded, so the total losses for three-winding loading would be not much greater than the H-L load loss at 1000 MVA. The impedances and losses averaged for the test results of 8 transformers are tabulated in Table III.

TABLE III
TRANSFORMER SHORT CIRCUIT FACTORY DATA

	Impedance (%)	*Power (MVA)*	*Loss (kW)*
HV-LV	15.8	1000	1764
HV-TV	117.2	1000 (60)	28677 (1720.62)
LV-TV	91.5	1000 (60)	29875 (1792.5)

Furthermore, the average no-load loss at rated voltage and frequency (measured on the tertiary) was 74.4 kW, whilst the average magnetizing current was 0.012% at 1000 MVA base.

Zero sequence data was not available and therefore zero sequence data that had been employed in this simulation model has been set equal to the positive sequence data. This is a reasonable assumption to make for a 5-limb core transformer with a tertiary winding. Provision of a tertiary winding on 5-limb cores drastically alters the zero sequence impedance, since zero sequence currents are able to circulate around the delta tertiary winding and thus balance those flowing into the primary winding [6].

Without a tertiary winding, the 5 limb core would have a higher zero sequence impedance (than the case where a tertiary winding is present) due to the 4^{th} and 5^{th} return limbs shunting the high reluctance zero sequence path (air path). The 4^{th} and 5^{th} return limbs of a 5 limb core are of much reduced section compared with the three main limbs. A zero sequence test at full load current would cause the 4^{th} and 5^{th} limbs to saturate and the core would turn into a 3-limb equivalent. In such a case the assumption of setting the zero sequence equal to the positive sequence data would not be valid.

III. ATP MODEL VERIFICATION

The circuit conditions described in section A of II, in terms of the disconnectors and circuit breakers status, were considered in the simulation model. Circuit breaker X_{420}, was utilized to carry out POW switching to initiate ferroresonance.

It should be noted that the circuit breaker X_{420} was tripped at a point in time (simultaneously for the three phases) that would ensure minimum voltages and energy transfer. This point has been marked as a reference point to start POW switching. Fundamental and subharmonic ferroresonance waveforms have been produced by simulation at a specific time. Table IV illustrates a comparison between the POW switching time corresponding to the field tests and to the simulation model. The ferroresonance voltage and current waveforms produced by simulation are also illustrated in Appendix I.

TABLE IV
P.O.W SWITCHING TIME COMPARISON

	Field Tests	**Simulation**	**Waveform Description**
POW switching control (time)	+3 ms	+3.2 ms	Subharmonic Mode
POW switching control (time)	+11 ms	+12.6 ms	Fundamental Mode

The following set of figures illustrates a comparison of a sector of the final steady state ferroresonance mode waveforms produced by ATP and those available from field recordings, for the fundamental and subharmonic case, for each one of the 3 phases (R, Y, and B).

Figures 4-9 compare the simulation results with the field results obtained for voltage and current corresponding to Phase R, Y and B respectively, for the fundamental mode ferroresonance.

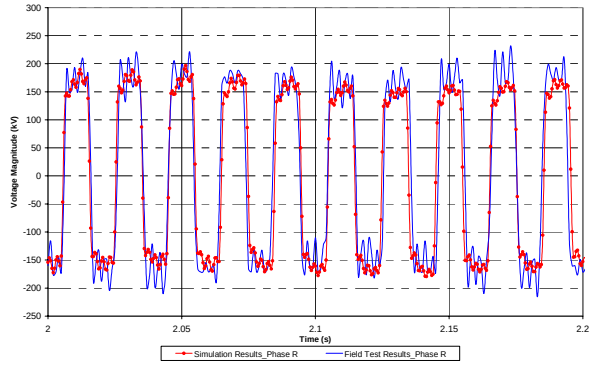

Fig. 4. Comparison of Fundamental Mode Ferroresonance- Section of Voltage waveform – R phase

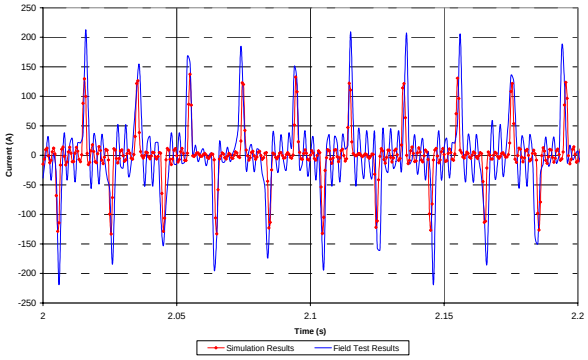

Fig. 5. Comparison of Fundamental Mode Ferroresonance- Section of Current waveform – R phase

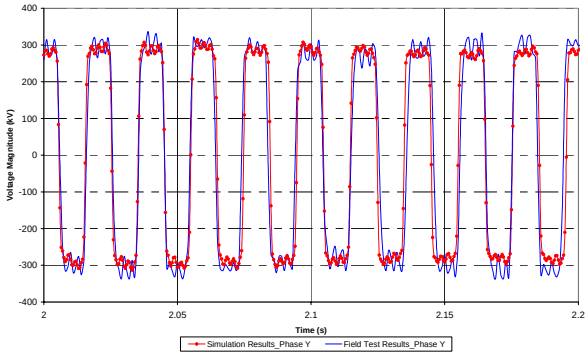

Fig. 6. Comparison of Fundamental Mode Ferroresonance- Section of Voltage waveform – Y phase

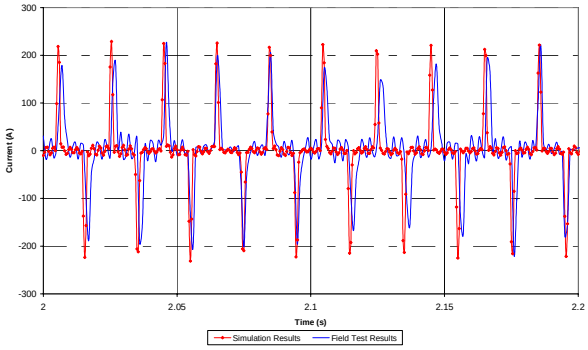

Fig. 7. Comparison of Fundamental Mode Ferroresonance- Section of Current waveform – Y phase

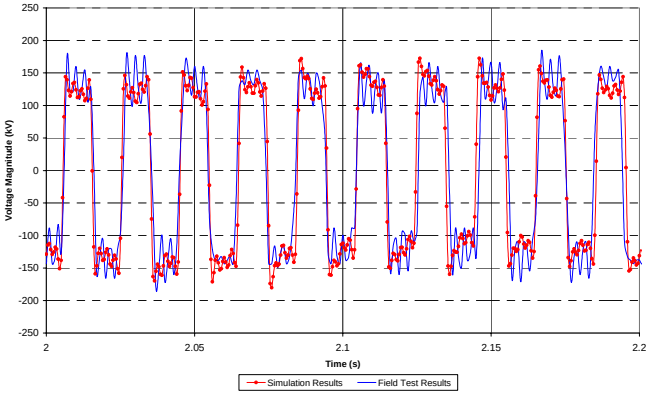

Fig. 8. Comparison of Fundamental Mode Ferroresonance- Section of Voltage waveform – B phase

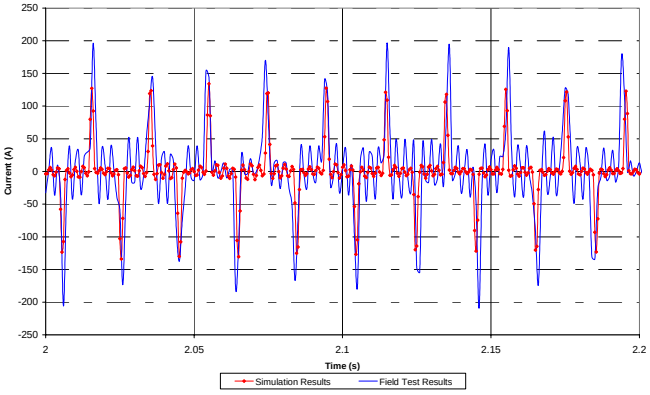

Fig. 9. Comparison of Fundamental Mode Ferroresonance- Section of Current waveform – B phase

Figures 10-15 compare the simulation results with the field results obtained for voltage and current corresponding to phase R, Y and B respectively, for the subharmonic mode ferroresonance.

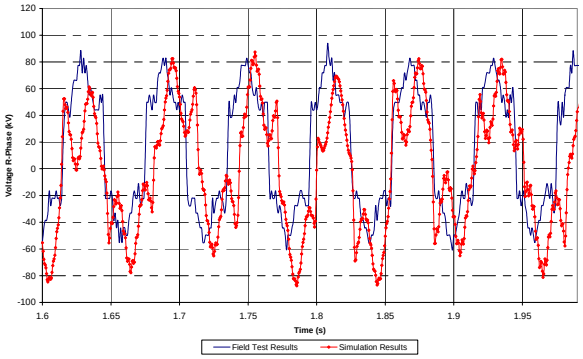

Fig. 10. Comparison of subharmonic Mode Ferroresonance- Section of Voltage waveform – R phase

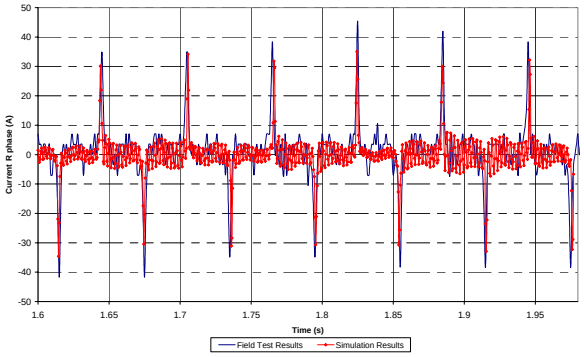

Fig. 11. Comparison of subharmonic Mode Ferroresonance- Section of Current waveform – R phase

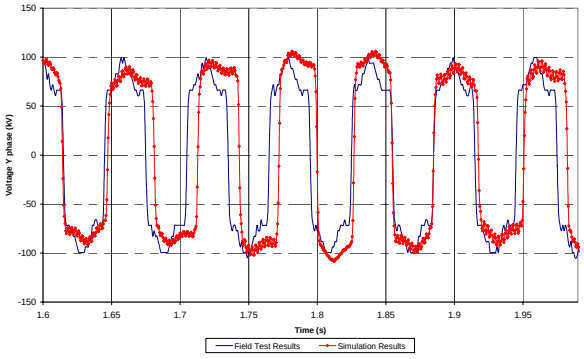

Fig. 12. Comparison of subharmonic Mode Ferroresonance- Section of Voltage waveform – Y phase

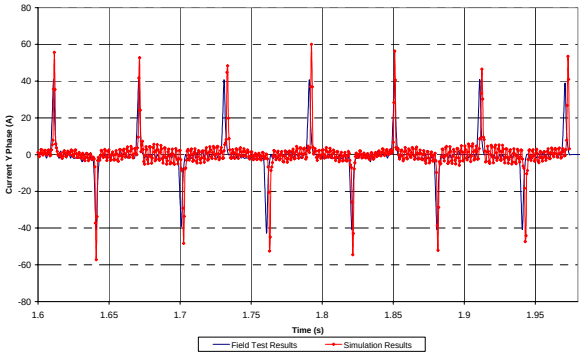

Fig. 13. Comparison of subharmonic Mode Ferroresonance- Section of Current waveform – Y phase

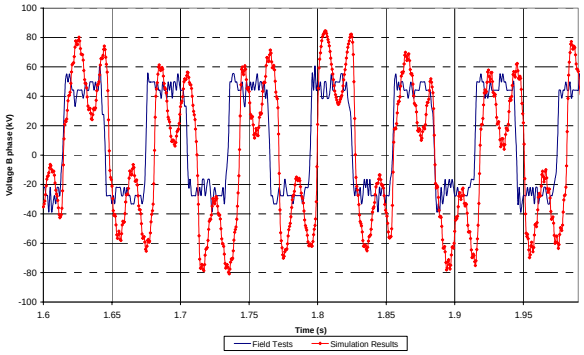

Fig. 14. Comparison of subharmonic Mode Ferroresonance- Section of Voltage waveform – B phase

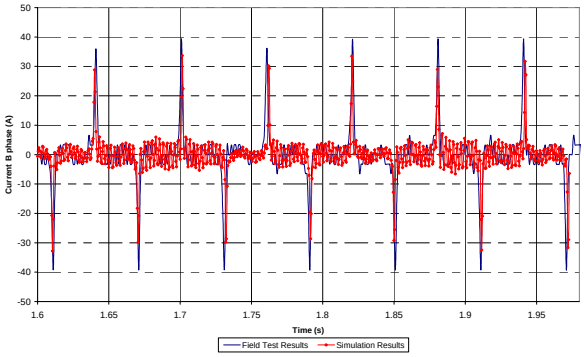

Fig. 15. Comparison of subharmonic Mode Ferroresonance- Section of Current waveform – B phase

The figures presented clearly illustrate that the ATP model can replicate the field recordings with a significant degree of accuracy, both in the fundamental and subharmonic case.

For the subharmonic case the ferroresonance condition had a frequency content of 16 $^{2/3}$ Hz. Table VI tabulates the peak and rms voltage and current values corresponding to field recordings and to simulation results.

TABLE V
COMPARISON OF FIELD AND SIMULATION RESULTS (FUNDAMENTAL)

	Field Test Results		Simulation Results (B)	
	Peak Voltage (kV)	RMS Volt. (kV)	Peak Voltage (kV)	RMS Volt. (kV)
R Phase	210	191	190	151
Y Phase	330	315	325	303
B Phase	180	173	190	167
	Field Test Results		Simulation Results	
	Peak Current (A)	RMS Cur. (A)	Peak Current (A)	RMS Cur. (A)
R Phase	200	62.56	145	46.45
Y Phase	220	70	220	70.52
B Phase	190	58.93	140	45.79

For the fundamental case the ferroresonance condition had a frequency content of 50 Hz. Table V tabulates the peak and rms voltage and current values corresponding to field recordings and to simulation results.

TABLE VI
COMPARISON OF FIELD AND SIMULATION RESULTS (SUBHARMONIC)

	Field Test Results		Simulation Results	
	Peak Voltage (kV)	RMS Volt. (kV)	Peak Voltage (kV)	RMS Volt. (kV)
R Phase	90	48.29	75	50.64
Y Phase	100	60	95	69.41
B Phase	50	37.06	45	41.05
	Field Test Results		Simulation Results	
	Peak Current (A)	RMS Cur. (A)	Peak Current (A)	RMS Cur. (A)
R Phase	45	9.28	35	5.6
Y Phase	42	8.997	50	9.3
B Phase	38	8.72	35	5.5

The minor differences on the voltage and current waveforms that appear on the illustrated Figures can also be seen on the frequency analysis waveforms illustrated by Figures 16 and 17, for the fundamental and subharmonic case respectively. Figures 16 and 17 compare the frequency content of voltage waveforms of the field recording results and the produced simulation results for one phase.

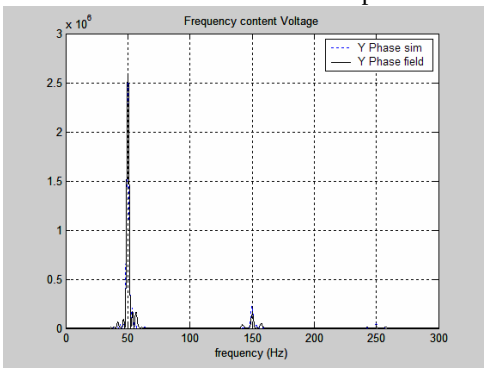

Fig. 16. Comparison of Frequency content of voltage waveforms (Fundamental –Y phase)

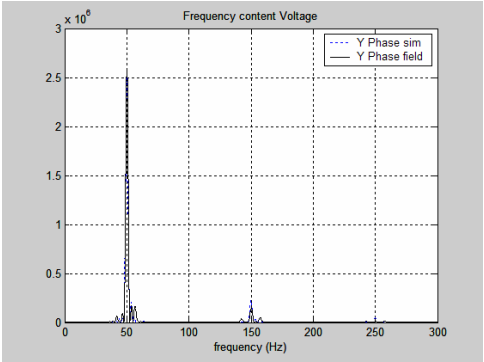

Fig. 17. Comparison of Frequency content of voltage waveforms (subharmonic – Y phase)

IV. CONCLUSIONS

Ferroresonance is a low frequency phenomenon that can occur when a transmission line connected to a transformer is switched out with the parallel circuit still energised. The complex UK network is such that a few power transformers are exposed to ferroresonance on mesh corner and circuit tee connections, mainly because of historical design precedents.

A reliable ATP based simulation model can be achieved when the parameters of the system and transformer are known or can be derived with reasonable accuracy. The graphical results presented in this paper clearly demonstrate the capability of the simulation model to reproduce the field recordings with a significant degree of accuracy, both in the fundamental and subharmonic case. The development and validation of this simulation model with the field recordings available allowed the authors to perform a number of sensitivity studies that deal with the effect on ferroresonance of point on wave (P.O.W) switching, transmission line and core losses and the interaction between these variables. The sensitivity studies investigate the effect the above described interactions have on energy transfer in the transformer, on the magnitude of ferroresonant voltages and currents and the duration of overvoltages, etc. The findings are the topic of a scientific paper submitted [3]. Lastly this simulation model will form the benchmark and will produce the input data of a detailed (topologically and geometrically accurate) transformer model that would enable the understanding of magnetic field analysis (heating and fluxing) within a transformer under ferroresonance and its degrading mechanisms.

V. Acknowledgement

The authors gratefully acknowledge the EPSRC – RAIS funding scheme and National Grid for the financial support. The authors also acknowledge the technical support provided by National Grid.

VI. References

[1] National Grid Seven Year statement 'Control of Ferroresonance' Technical Guidance Note, December 2004, National Grid, UK, www.nationalgrid.com/sys

[2] ATP Rule Book and Theory Book, Can/Am EMTP User Group, Portland, OR, USA, 1997.

[3] C. Charalambous, ZD Wang, Mark Osborne, Paul Jarman, '' Sensitivity studies on a power transformer model for ferroresonance on a 400 kV Circuit. IET Proceedings in Generation, Transmission and Distribution (Under Review)

[4] 'Ferroresonance Tests on Brinsworth-Thorpe Marsh 400 kV circuit', Technical Report TR (E) 389, Issue 1, July 2001, National Grid, UK..

[5] Juan A. Martine-Velasco, Bruce A. Mork, ''Transformer Modeling for Low Frequency Transients – The state of the Art, IPST 2003 New Orleans, USA.

[6] A.C Franklin, D.P Franklin, The J&P Transformer Book, 12th Revised edition , Elsevier Science & Technology

[7] British Electricity International, Modern Power Station Practice, EHV Transmission, Volume K, Pergamon Press

VII. Appendix

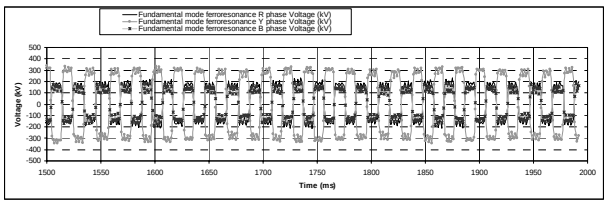

Fig. 18. Fundamental Mode Ferroresonance – Voltage (Field Recordings)

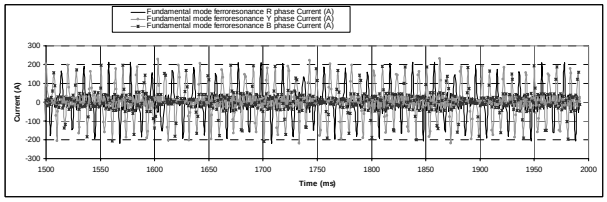

Fig. 19. Fundamental Mode Ferroresonance – Current (Field Recordings)

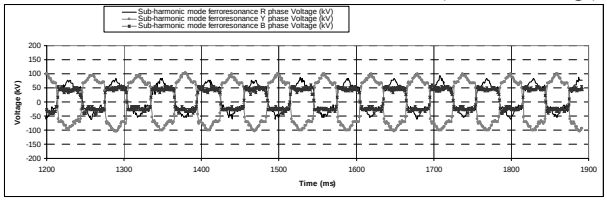

Fig. 20. Subharmonic Mode Ferroresonance – Voltage (Field Recordings)

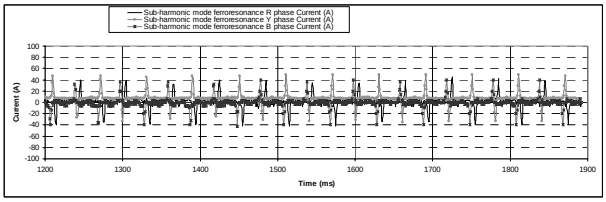

Fig. 21. Subharmonic Mode Ferroresonance – Current (Field Recordings)

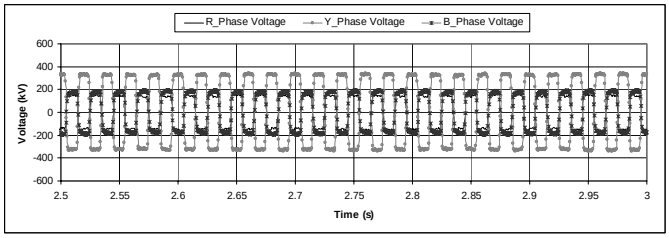

Fig. 22. Fundamental Mode Ferroresonance – Voltage (Simulation Results)

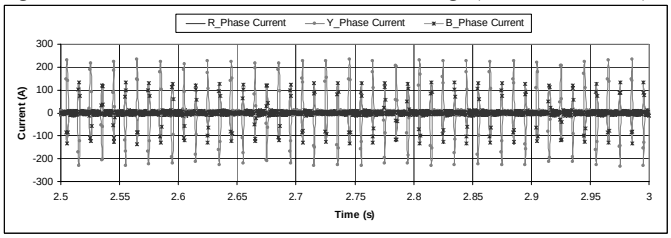

Fig. 23. Fundamental Mode Ferroresonance – Current (Simulation Results)

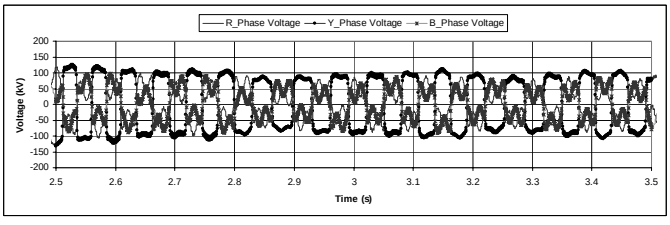

Fig. 24. Subharmonic Mode Ferroresonance – Voltage (Simulation Results)

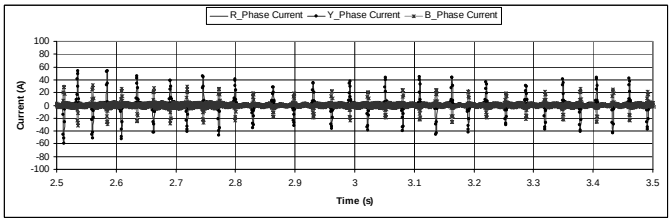

Fig. 25. Subharmonic Mode Ferroresonance – Current (Simulation Results)